RADIATION HYDRODYNAMICS OF ACCRETING MAGNETIC WHITE DWARFS

K. BEUERMANN, U. WOELK
Univ.-Sternwarte, Geismarlandstr. 11, 37083 Göttingen, FRG

Abstract. We solved the stationary one-dimensional two-fluid radiation hydrodynamic equations including cyclotron radiation for a wide range of mass flow rates. Here, we discuss the implications for accretion phenomena on the white dwarfs in AM Her binaries.

1. Introduction

In accreting magnetic white dwarfs, the atmosphere is heated by a stream of free falling protons. If the mass flow rate is low, $\dot{m} \leq 10^{-1}\,\mathrm{g\,cm^{-2}s^{-1}}$, the protons lose their energy by Coulomb encounters with atmospheric electrons and the energy is radiated within the stopping length (bombardment case, Kuijpers & Pringle 1982). For high mass flow rates, a hydrodynamic shock forms and the energy is radiated from the extended post-shock cooling region. The radiative transfer problems for the bombardment (non-hydrodynamic) case and for the hydrodynamic case were solved by Woelk & Beuermann (1992, 1993, hereafter WB92, WB93) and by Woelk & Beuermann (1996, hereafter WB96), respectively. We discuss the implications of these results for the study of AM Her binaries.

2. Computational method and results

WB96 solved the stationary one-dimensional two-fluid viscous hydrodynamic equations simultaneously with the fully frequency and angle dependent radiative transfer, including anisotropic cyclotron absorption. The connecting link between the hydrodynamic and the radiative transfer equations is the radiative flux; its gradient balances the energy loss of the settling matter. We obtained solutions for wide ranges of the mass flow rates and field strengths, $\dot{m} = 10^{-3} \ldots 10^{2}\,\mathrm{g\,cm^{-2}s^{-1}}$ and $B = 5 \ldots 70\,\mathrm{MG}$. The

A. Evans and J. H. Wood (eds.), Cataclysmic Variables and Related Objects, 199–202.

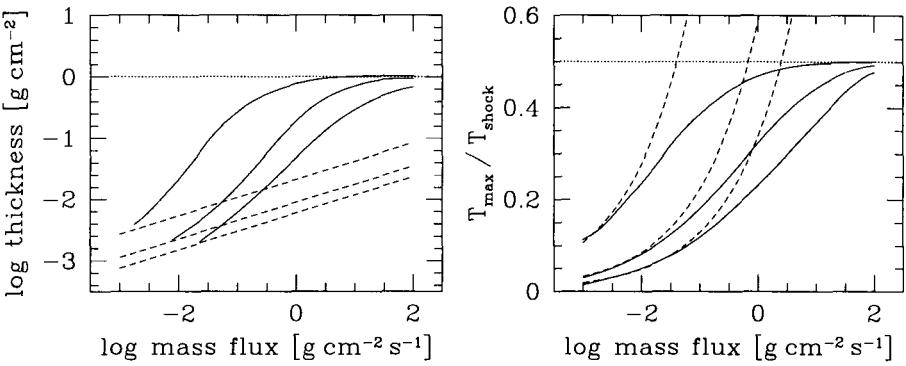

Figure 1. Maximum post-shock electron temperature and thickness of the cooling region for a white dwarf mass $M_{wd} = 0.7\,M_\odot$ and magnetic field strengths $B = 10, 30$, and 50 MG (from top); zero-field case (dotted line); bombardment case (dashed curves).

electron temperature behind the shock is determined by the competition between Coulomb collisions with the ions and radiative losses; the maximum temperature achieved decreases with decreasing $\dot{m}$ and increasing B. At the same time, the thickness (column density) of the flow collapses by up to 3 orders of magnitude below that of the zero-field case due to the increasing cyclotron losses. Fig. 1 depicts some results from WB96 for a white dwarf mass of $0.7\,M_\odot$ and field strengths of 10, 30, and 50 MG, along with the zero-field case. For low $\dot{m}$ and high B, the temperature distribution and cooling lengths approach those of the bombardment case (dashed curves; WB92). The transition occurs between 10^{-3} and $10^{-1}\,\mathrm{g\,cm^{-2}s^{-1}}$ for field strengths of 10 to 70 MG. For higher flow rates, the bombardment solution becomes invalid and the hydrodynamics must be taken into account.

For comparison with observations, the geometric height, h, of the cooling region is also of interest (Fig. 2). This is the stand-off distance of the shock above the bottom of the cooling flow. As noted by Beuermann (1988) and Stockman (1988), the bottom of the flow at h_{ram} (i.e. $p = p_{ram}$, where p_{ram} is the ram pressure) is increasingly pushed into the atmosphere and the formation of trenches will affect the escape of the radiation. We determine the trench depth, d, relative to some reference level, h_N, in the atmosphere which we took to correspond to a residual atmospheric column density, $N_H = 10^{23}$ H-nuclei cm^{-2}. If the shock drops below this level, bremsstrahlung may be considered effectively trapped, because it can neither escape sideways nor through the high column density of the pre-shock flow. For an isothermal atmosphere with effective temperature T_{eff} given by $\sigma T_{eff}^4 = GM_{wd}\dot{m}/R_{wd}$, the atmospheric scale height is $H = kTR_{wd}^2/m_H GM_{wd}$ and $d = h_N - h_{ram} = H\ln(p_{ram}/p_N)$, where $p_N = GM_{wd}m_H N_H/R_{wd}^2$. Fig. 2 shows that d exceeds h for $\dot{m} > 30\,\mathrm{g\,cm^{-2}s^{-1}} \simeq \frac{1}{3}\dot{m}_{Edd}$. Finally, we comment on the geometry of the cool-

https://doi.org/10.1017/S0252921100038616 Published online by Cambridge University Press

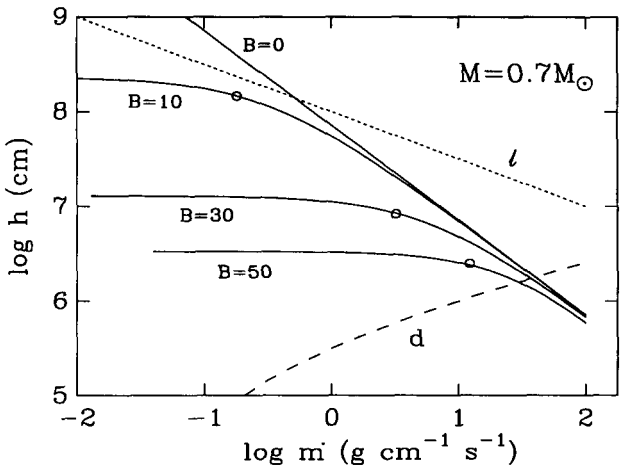

Figure 2. Shock height (cooling length) as a function of the mass flow rate for $M_{\rm wd} = 0.7\,{\rm M}_\odot$ and field strength of 0, 10, 30, and 50 MG. Also shown is the depth, d, of the pressure-induced trench and a typical linear extent, l, of the accretion spot for $\dot{M} = 10^{16}$ g s^{-1}. All curves terminate at $\dot{m}_{\rm Edd} = 75\,R_9^{-1}$ g cm^{-2}s^{-1} $\simeq 100$ g cm^{-2}s^{-1}.

ing region by comparing its linear extent, l, with the stand-off distance, h. For a typical accretion rate $\dot{M} = A\dot{m} = 10^{16}$ g s^{-1} and $A = l^2$, we have $l = (\dot{M}/\dot{m})^{1/2}$ (Fig. 2, dotted line). In the zero-field case, $h > l$ for low $\dot{m}$ and the emission region becomes tall. For the larger $B-$values, however, $h \ll l$ and the region as a whole is rather pill-box shaped.

3. Discussion and conclusion

Our present results are important for an understanding of the cyclotron and bremsstrahlung emission from magnetic CVs. The observed accretion spots in AM Her binaries display internal structure with a large range of $\dot{m}$ (e.g. Beuermann, Stella & Patterson 1987), often referred to as core-halo structure. The low-$\dot{m}$ halo produces part of the observed cyclotron emission including the optically thin cyclotron lines while the core(s) produce(s) the bremsstrahlung and an underlying cyclotron continuum. The theory allows us to interpret a given cyclotron spectrum in terms of B *and* of the range of peak temperatures or of the flow rates which contribute to this spectrum. For AM Her binaries with pronounced cyclotron lines (as e.g. UZ For; Beuermann, Thomas & Schwope 1988) a fit by theoretical cyclotron spectra implies that a range of $\dot{m}$ values is present, e.g. from 10^{-3} to 10^{-1} g cm^{-2}s^{-1} for UZ For (Rousseau et al. 1996). The fraction of the accretion energy released as bremsstrahlung is very low at these low $\dot{m}$-values and values of the order of $\dot{m} = 10$ g cm^{-2}s^{-1} are needed to account for the hard X-ray emission seen in some systems in their high states.

https://doi.org/10.1017/S0252921100038616 Published online by Cambridge University Press

Beuermann & Schwope (1994) have demonstrated that bremsstrahlung is systematically suppressed at high B. Fig. 2 provides a hint why this may be so. Following Beuermann et al. (1987) we assume that the accretion stream stagnates in the outer magnetosphere at a point where $B^2/4\pi = m_{\rm H} n\, v^2$. To a first approximation, n will equal the particle density in the line-emitting region. Following the dipole lines, this matter arrives at the surface of the white dwarf with mass flow rate $\dot{m} = B(m_{\rm H} n/4\pi)^{1/2} = 36 B_7 n_{14}^{1/2}$, where B_7 and n_{14} are the surface field strength and the particle density in the stagnation region in units of 10^7 G and $10^{14}\,{\rm cm}^{-3}$, respectively. For $n = 10^{13} \ldots 2\,10^{14}$ cm^{-3} (Liebert & Stockman 1985), $\dot{m}$ ranges from $10 \ldots 50$ and from $50 \ldots 250\,{\rm g\,cm^{-2}s^{-1}}$ for $B_7 = 1$ and 5, respectively. This is the material which produces the dense accretion cores. With increasing B, this material is driven further into the region where shocks tend to be covered up. In fact, for $B_7 = 3$, where bremsstrahlung starts to be significantly suppressed, the above $\dot{m}$-range has just moved entirely to the right of the intersection of solid and dashed line in Fig. 2. At the same time the output in soft X-rays will increase. To be sure, our radiation hydrodynamic calculations do not bear directly on the open problem of how the intense soft X-ray emission from AM Her binaries is produced. A formal solution of the so-called 'soft X-ray puzzle' requires the time-dependent treatment of the hydrodynamics simultaneously with an appropriate two-dimensional radiative transfer (because edge effects are important). It will also be important to include the radiation pressure in the hydrodynamics and heat conduction in the energy transport, both of which were neglected in the calculations of WB96. Such calculations are not presently available. The above example suggests, however, that even in the stationary case increasing field strength implies a suppression of the bremsstrahlung flux which is likely to be reprocessed into soft X-rays.

References

Beuermann, K., Stella, L., Patterson, J., 1987, Ap. J., **316**, 360
Beuermann, K., 1988, in "Polarized Radiation of Circumstellar Origin", eds. G.V. Coyne et al., University of Arizona Press, p125
Beuermann, K., Thomas, H.-C., Schwope, A.D., 1988, A&A, **198**, L15
Beuermann, K., Schwope, A.D., 1994, in "Interacting Binary Stars", ed. A. Shafter, ASP Conf. Ser. **56**, 119
Kuijpers, J., Pringle, J.E., 1982, A&A, **114**, L4
Liebert, J., Stockman, H.S., 1985, in "Cataclysmic Variables and Low-mass X-ray Binaries", eds. D.Q. Lamb, J. Patterson, Reidel Publ. Co.
Rousseau, T., Fischer, A., Beuermann, K., Woelk, U., 1996, A&A, in press
Stockman, H.S., 1988, in "Polarized Radiation of Circumstellar Origin", eds., G.V. Coyne et al., University of Arizona Press, p237
Woelk, U., Beuermann K., 1992, A&A, **256**, 498 (WB92)
Woelk, U., Beuermann K., 1993, A&A, **280**, 169 (WB93)
Woelk, U., Beuermann K., 1996, A&A, **306**, 232 (WB96)